Radiocarbon, Vol 64, Nr 1, 2022, p 171–186 DOI:10.1017/RDC.2021.100

COMPARING ANALYSIS OF PRETREATMENT METHODS OF WOOD AND BONE MATERIALS FOR THE CHRONOLOGY OF PERIPHERAL BURIALS AT TUNNUG 1, TUVA REPUBLIC, RUSSIA

Fatima Pawełczyk[1]* • Irka Hajdas[2] • Timur Sadykov[3] • Jegor Blochin[3] • Gino Caspari[4,5]

[1]Silesian University of Technology, Gliwice 44-100, Poland
[2]ETH - Laboratory of Ion Beam Physics, HPK H25, Otto-Stern-Weg 5, Zurich 8093, Switzerland
[3]Institute of History of Material Culture of the Russian Academy of Sciences, St. Petersburg, Russia
[4]The University of Sydney, Sydney, New South Wales, Australia
[5]University of Bern, Bern, Switzerland

ABSTRACT. Nine burials from Tunnug 1 site in Tuva Republic, which contained human and animal bones as well as remains of wood, were chosen for intercomparison study of preparation methods. Nine human bones, nine animal bones and 11 pieces of wood were prepared. Gelatin extracted from bones was purified using the UF method but the extraction from bones was modified with respect to acid and base treatment. Wood samples were treated as whole using acid-base-acid and cellulose was extracted for comparison. The results confirmed a highly consistent chronology of the sites centered at 200–400 CE, however, a few bones resulted in an offset between ages obtained by different methods. The extraction of cellulose was limited due to the poor preservation of wood. Our results highlight problems of dating poorly preserved bones and wood.

KEYWORDS: burial mound, radiocarbon AMS dating, Tunnug, Tuva, ultrafiltration.

INTRODUCTION

Archaeologists often face choices when sampling archaeological materials for radiocarbon (^{14}C) dating. Charcoal, wood, and bone are the most commonly analyzed material when dating archaeological contexts. Human bones when ^{14}C dated are usually expected to date closely to the event of burial and thus provide an estimate for the usage of the archaeological site, provided no food reservoir age exists. However, ^{14}C ages of bones must be evaluated carefully with respect to potential contamination and treatment efficiency. Bone is not a perfectly closed system to the carbon exchange. When buried in soil for centuries or millennia, bones are exposed to humic acids, a potential source of exogenous carbon. The age offset from the accurate ^{14}C age is dependent on the geochemistry of the burial, the age of the bones, their preservation, and the age of exogenous carbon. Numerous treatment methods have been designed to remove such contamination. A variety of approaches appeared over the decades (for an overview see Herrando-Pérez 2021). The most common are the Longin method (Longin 1971) and ultrafiltration (Brown et al. 1988), which are often modified by laboratories (Piotrowska and Goslar 2002; Brock et al. 2007; Hajdas et al. 2009; Brock et al. 2010; Wood 2015). Other methods involve separation and dating of specific bone components such as peptides using a ninhydrin reaction with amino acids (Nelson 1991) or a chromatographic separation of hydroxyproline (McCullagh et al. 2010; Marom et al. 2012; Deviese et al. 2018). Intercomparisons performed between various laboratories (Scott et al. 2010) are a way to test the different methods. Limited comparisons are often carried out as part of research projects (Fiedel et al. 2013; Huels et al. 2017; Kuzmin et al. 2018; Quarta et al. 2021).

*Corresponding author. Email: fatima.pawelczyk@polsl.pl
This article has been updated since its original publication. See https://doi.org/10.1017/RDC.2021.117.

The treatment of wood for radiocarbon dating can be either performed by acid-base-acid protocol (ABA or AAA) or separation of cellulose (Brock et al. 2010; Nemec et al. 2010a; Southon and Magana 2010; Hogg et al. 2013; Hajdas et al. 2017). The treatment is chosen depending on sample size and preservation of cellulose. Applications such as high-resolution radiocarbon dating of large, well preserved wood fragments, for example for calibration purpose or environmental studies of trees, involve cellulose separation. However, waterlogged/wet wood has little cellulose left (Hajdas et al. 2017) and samples smaller than 10 mg (dry), even well preserved but ones, have little prospect to provide sufficient amount of cellulose. Such samples are therefore only treated with ABA i.e., as whole wood sample.

In this study we analyze commonly available archaeological materials—animal bone, wood, and human bone—from a site in southern Siberia. In order to understand the chronology of events on site, it is essential to develop a ^{14}C chronology. Moreover, most burial pits contain coffin wood and animal bones from meat offerings for the dead. This provides an opportunity to study potential differences between ^{14}C ages of different types of material. For this purpose, nine burials with sets of samples containing wood, human, and animal bones were chosen for ^{14}C analysis by AMS.

The preparation for ^{14}C dating of bones has been extensively discussed in the literature (Higham et al. 2006; Fuller et al. 2014; Herrando-Pérez 2021). The most common discussion is dedicated old bones yielding ^{14}C dates which are younger than expected (e.g., Higham et al. 2006). However, occasionally ages of relatively young bones appear to be affected in a similar way (Heinemeier et al. 2013; Rubinetti et al. 2020). While comparing results of different material pretreatments, possible offsets due to reservoir ages due to marine and fresh water components of the diet (Sveinbjörnsdóttir et al. 2010) should be considered. Also, there is a possibility of the "old wood" effect, when ^{14}C dating of cremated bones and associated context samples (Olsen et al. 2013). Our goal was to compare the effect of two bone pretreatment protocols, differing in terms of chemical preparation, but each included an ultrafiltration step. We also compared the results of dating two sets of wood samples—subjected to standard ABA preparation and separation of cellulose. Here we present the results obtained using different preparation techniques and discuss consequences for the detailed chronology of the Tunnug 1 site.

MATERIAL AND STUDY SITE

The joint Russian-Swiss excavation project at Tunnug 1 in Tuva Republic was kicked off through a preliminary survey in 2017. A site in the floodplain of the Uyuk River was identified (Figure 1), analyzed by means of remote sensing data and ultimately visited.

During this first field research campaign, a large Early Iron Age burial mound in the Uyuk Valley in southern Siberia was meticulously mapped by means of photogrammetry and small test excavations provided a first idea of the chronological setting of the site (Caspari et al. 2018). A massive stone mound with several dozen buried individuals, many of whom died a violent death, was uncovered in 2019 (Milella et al. 2021). The ^{14}C dates from larch wood recovered from the test excavations indicated a date for the construction of the burial mound in the 9th century BCE, this was later confirmed through additional ^{14}C dates in combination with dendrochronology (wiggle matching) (Caspari et al. 2020a). Despite a large number of monumental burial mounds in the Uyuk Valley dating to the Early Iron Age (Caspari 2020; Caspari et al. 2020b), few are chronologically situated in the Late

https://doi.org/10.1017/RDC.2021.100 Published online by Cambridge University Press

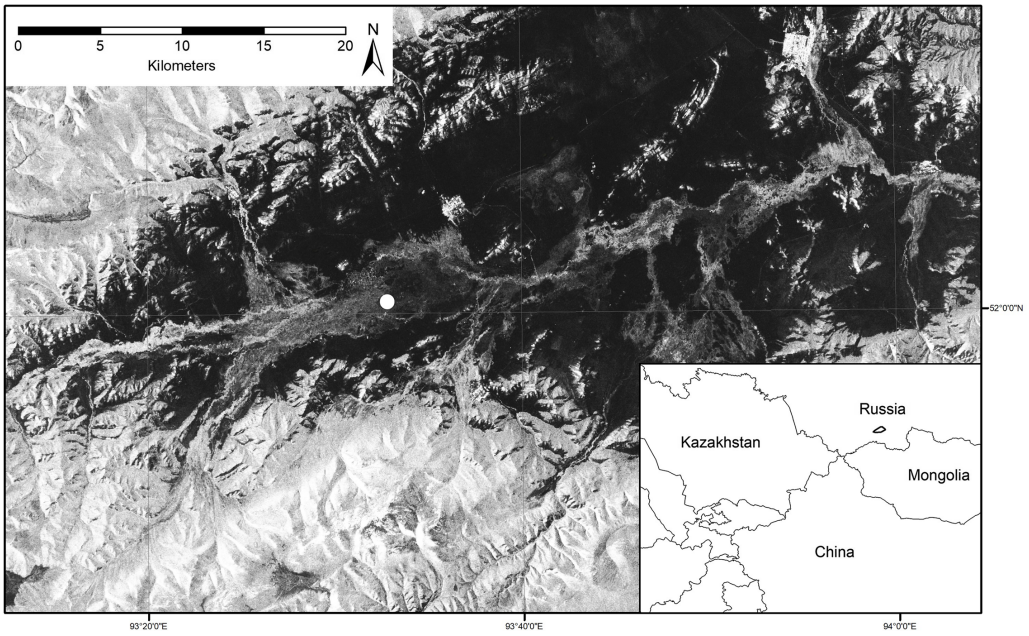

Figure 1 The site location (indicated with a white spot) in the Uyuk Valley in southern Siberia, Tuva Republic, Russian Federation.

Bronze Age Early Iron Age transition and are relevant to understanding the economic and cultural shifts happening in the first part of the first millennium BCE (Sadykov et al. 2020).

The analysis of the burial mound's immediate periphery through remote sensing and geophysical surveys showed that the burial mound is not an isolated architectural site but rather surrounded by dozens of smaller ritual and burial structures (Caspari et al. 2019). Already in 2018 an amorphous barrow was identified in the southern periphery, under which numerous burial pits were located (Sadykov et al. 2019). Most of them date to the 2nd–4th century CE and belong to the Kokel culture (Milella et al. 2021; Sadykov et al. 2021). These burial pits contain partially preserved wooden coffins, well-preserved human bones, as well as meat offerings remaining in the form of animal bones. Figure 2 provides an overview over the archaeological structures in the southern periphery from which the samples for this study stem.

Initial samples of human bone and wood were radiocarbon dated by LARA-Bern laboratory as a part of previous studies (Milella et al. 2021). The material selected for radiocarbon dating for this study came from nine burial pits under a large amorphous stone accumulation in the southern periphery of the Tunnug 1 site. ^{14}C dating was performed based on 32 bone samples (14 samples from animal bones and 18 samples from human bones) as well as 22 wood samples (11 of which were in the form of cellulose).

METHODS

All the steps and details of each of the pretreatment methods used are summarized in Table 1. We used two different preparation protocols for the bone material UF1 and UF2. Wood

https://doi.org/10.1017/RDC.2021.100 Published online by Cambridge University Press

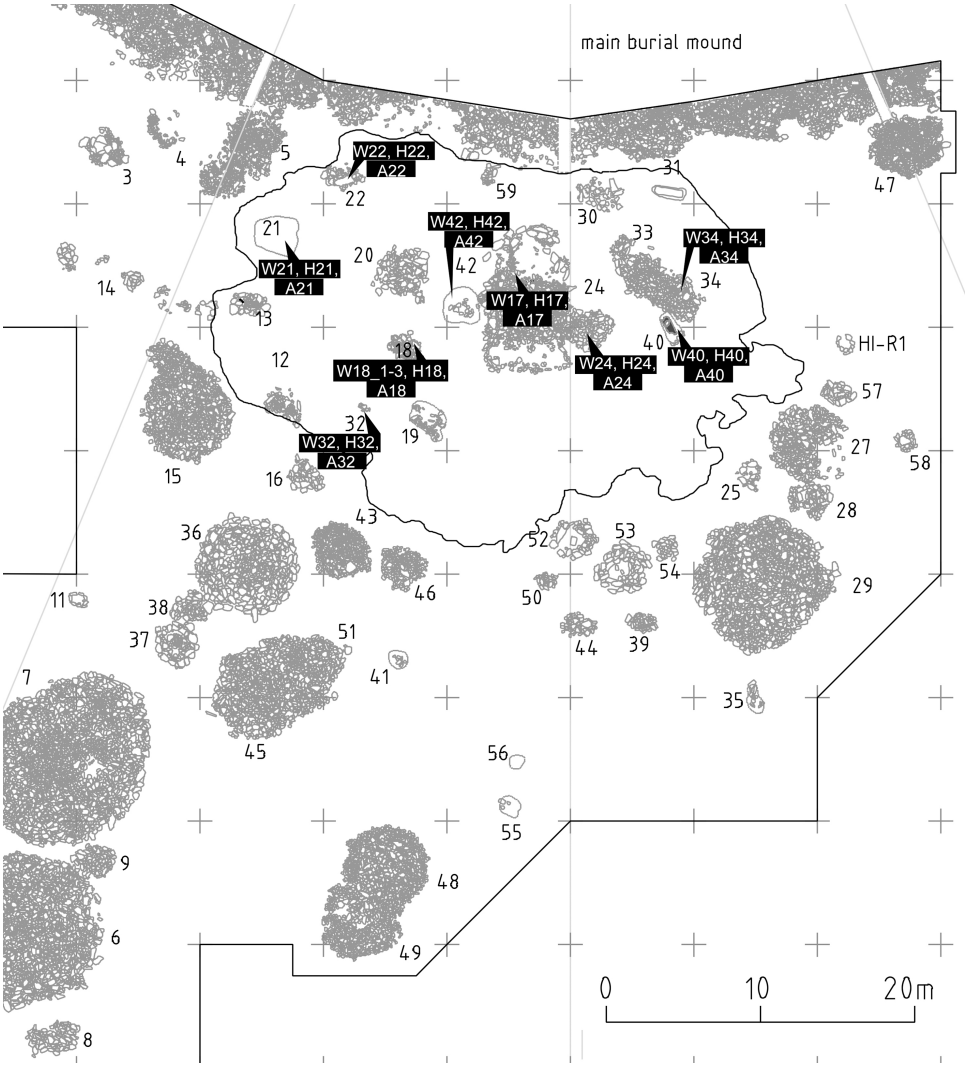

Figure 2 The southern periphery of the Tunnug 1 site: numbers indicate the archaeological structures; the black outline marks the boundaries of the amorphous stone mound; black labels indicate where the samples stem from. Samples are numbered and labelled with W (wood), H (human bones), and A (animal bones).

samples were treated following a standard acid-base-acid (ABA) protocol or using cellulose extraction (BABAB) (Nemec et al. 2010a).

Preparation of Bones

Radiocarbon analysis of osteological material is performed on extracted gelatine. The first step of preliminary chemical preparation was the same for all samples and included cleaning in an ultrasonic bath in demineralised water (2×15 min), drying, then grinding in metal mortars, pulverizing and subsequently sieving on metal sieves (<710 μm).

https://doi.org/10.1017/RDC.2021.100 Published online by Cambridge University Press

Table 1 Summary of preparation steps. For bone samples, two ultrafiltration protocols were used (UF1, UF2), preceded by a modified Longin's method; for wood, standard protocol (ABA) and pretreatment with cellulose extraction (BABAB) were applied. RT = room temperature (20°C).

Treatment code	Demineralization	Alkali wash	Gelatinization	Filtration	Ultrafiltration
UF1	0.5 M HCl, 1–2 hr, RT	0.1 M NaOH, 30 min, RT	pH 2, >17 hr, 100°C	MillexGlasfaser filter	Amicon Ultrafilter centrifuge 4400 rpm, 5–20 min
UF2	1.1 M HCl, 3 × 2 hr, RT	0.1 M NaOH, 30 min, RT	pH 3, 20 hr, 60°C	MillexGlasfaser filter	Amicon Ultrafilter centrifuge 4400 rpm, 5–20 min
	Acid wash	Alkali wash	Acid wash		
ABA	0.5 M HCl, 1 hr, 60°C	0.1 M NaOH, 1 hr, 60°C	0.5 M HCl, 1 hr, 60°C	—	—
	Alkali wash	Acid wash	Alkali wash	Acid wash	Cellulose extraction
BABAB	1 M NaOH, overnight, 60°C	1 M HCl, 0.5 hr, 60°C	1 M NaOH, 1.5 hr, 60°C	1 M HCl, 10 min, RT	5 mL of 0.6 M NaClO2, 200 µL of 1 M HCl, pH 3

Aliquots of a few milligrams of original bone were wrapped in Sn boats to obtain the carbon and nitrogen quantities (%C, %N, C/N_{at}) with the Elemental Analyzer (Vario MicroCube, Elementar), which was calibrated using Acetanilide as a reference material. The levels of carbon and nitrogen (%C and %N) in raw bones were in the order of ca. 15–18% and 4–6%, respectively, in each case suggesting good collagen preservation (DeNiro 1985; Ambrose 1990; van Klinken 1999).

Every sample of bone powder was divided into two, in order to compare different gelatinisation protocols. Some of the samples were too small so in those cases we left just one—there are no comparable results for A18, A21, A24 and A32 samples. Finally, 32 subsamples of bone were tested—18 subsamples of human bone and 14 subsamples of animal bone.

Two sets of samples were subjected to the pretreatment protocol based on a modified Longin's method (Longin 1971; Arslanov and Svezhentsev 1993), combined with ultrafiltration. All the samples containing ~1 g of powder <710 µm were placed in 50 mL Falcon tubes. These steps include the following order: demineralisation, alkali treatment, gelatinisation, filtration and ultrafiltration. Batch one which contained 18 samples, underwent treatment UF1 and batch 2 with 14 samples underwent treatment UF2 (Table 2).

https://doi.org/10.1017/RDC.2021.100 Published online by Cambridge University Press

Batch 1 (UF1) was treated with 0.5 M HCl for a period of minimum 20 mins at room temperature to remove the mineral fraction. When no bubbles were visible in the solution, the reaction was considered complete. In most cases, the time required for full demineralisation was longer and ranged from one to two hours. After rinsing with ultrapure water, the samples were treated with base-sodium hydroxide (0.1 M NaOH, 30 mins, room temperature). Next, they were rinsed with ultrapure water to neutral pH and then with 0.001 M HCl. The next step was gelatinisation in an acidic solution (HCl, pH=2) in 100°C for at least 17 hr.

Batch 2 (UF2) was prepared according to second protocol. The first step of demineralisation was performed with 1.1 M HCl for 2 hr at room temperature. That step was repeated three times to ensure that all of the mineral fraction had reacted. Next, the samples were left overnight in ultrapure water with a drop of acid. The next day, after rinsing with ultrapure water to neutral pH, the samples were treated with 0.1 M NaOH for 30 min at room temperature to remove humic acids and rinsed again. Then the samples were treated with 1.1 M HCl, then rinsed with ultrapure water and then with 0.001 M HCl. The gelatinisation step was performed for 20 hr at 60°C (pH=3). All the gelatinised samples were subsequently subjected to filtration through precleaned Millex Glasfaser filters. All gelatine sample fractions were placed in Millipore Amicon Ultra-15 ultrafiltration tube, precleaned following the protocol of Brock et al. (2007). Subsequently, the samples were centrifuged at 4400 rpm for 5–20 min to remove the fraction <30 kD to collect the heavy-molecule fraction >30 kD (Hajdas et al. 2009). Then, purified gelatine samples were freeze-dried (Alpha 1-2 LD plus, Martin Christ).

Preparation of Wood

11 wood samples (Table 2) were divided into two subsets, to obtain 22 subsamples. One set of 11 subsamples was subjected to ABA—acid-base-acid (or AAA—acid-alkali-acid) preparation, used since the 1950s (de Vries and Barendsen 1954) and now widespread in radiocarbon laboratories. An acid-base-acid preparation of was carried out at 60°C, as follows: 0.5 M HCl for 1 hr for removing carbonate contaminants; after rinsing with ultrapure water, a bath in 0.1 M NaOH for 1 hr dissolved humic acids; next, after rinsing with ultrapure water, 0.5 M HCl was applied for 1 hr, to remove a possible contamination with modern carbon; a final step was rinsing with ultrapure water to neutral pH. Hereafter we will refer to this set as "ABA."

The second set of wood subsamples was converted into cellulose, to compare the results. The set of wood samples was treated according to standard ETH protocol, called BABAB (Nemec et al. 2010a) with base, acid, base (1 M NaOH, overnight; 1 M HCl, 0.5 hr; 1 M NaOH, 1.5 hr), at 60°C. Next, the samples were briefly (10 min, RT) exposed to 1 M HCl and then a solution of 5 mL of 0.6 M $NaClO_2$ and 200 µL of 1 M HCl was added to every sample. Next step was rinsing the samples. Some of them were very tough to rinse after NaOH, some of them dissolved partially in alkali solution and W34 (ETH-105167) dissolved completely. The samples needed to be centrifuged while rinsing (2500 rpm, 3 min). Every sample of wood and cellulose was freeze-dried after chemical preparation.

After chemical pretreatment both UF1 and UF2 gelatine batches as well as ABA and Cellulose sets were subjected to graphite preparation using an AGE-3 system, equipped with an

https://doi.org/10.1017/RDC.2021.100 Published online by Cambridge University Press

Table 2 Results for ^{14}C comparison of UF1, UF2, W1, and W2 batches of samples, with mean values, from nine areas of the Tunnug 1 site. Sample yield and mg C (target); weight percent of C and N in original bones as well as C/N atomic ratios (C/N_{at}) for gelatine samples. Previous results from Milella et al. (2021). Sample lost during pretreatment marked with an asterisk (*).

	This study													Milella et al. (2021) (all human bones but one)
Area	ETH lab code	Sample code	Material	Treatment	Sample yield, %	%N in raw bone	%C in raw bone	%N in gelatin	%C in gelatin	mg C	C/N_{at}	^{14}C age BP	± 1σ	^{14}C age BP ± 1σ
	105147	W17	Wood	ABA	70					0.99		1709	23	
				Cellulose	17					1		1711	23	
				mean								***1710***	***16***	
17	105148	H17	Human bone	UF1	9	5.17	16.59	15.6	43.9	1	3.3	1825	22	1787 ± 20
				UF2	7			15.8	43.4	1	3.2	1815	24	1738 ± 20
				mean								***1820***	***16***	
	105149	A17	Animal bone	UF1	1	4.66	15.9	13.7	37.5	1	3.2	4219	27	
				UF2	5			13.6	37	1	3.2	4169	27	
				mean								***4194***	***19***	
	105150	W18_1	Wood	ABA	27					0.99		1724	23	
				Cellulose	1					0.32		1860	24	
				mean										
			Wood/ rootlets									*3447*	*426*	
	105151	H18	Human bone	UF1	4	4.9	16.52	11.9	32.8	1	3.2	1763	24	1743 ± 20
				UF2	2			16.4	44.3	1	3.2	1744	24	
				mean								***1753***	***17***	
18	105152	A18	Animal bone	UF1	3	3.76	14.82	13.2	39.6	0.99	3.5 *poor C/N*	*1839*	*22*	
	105153	W18_2	Wood	ABA	13					0.65		1755	23	
				Cellulose	13					0.85		1847	23	
				mean										
	105154	W18_3	Wood	ABA	50					0.99		1780	23	
				Cellulose	4					1		1842	23	
				mean								***1812***	***16***	
	105155	H21	Human bone	UF1	12	5.48	17.47	15.3	42.7	0.99	3.3	1784	22	
				UF2	8			15.5	42.4	0.99	3.2	1796	24	
				mean								***1789***	***16***	

(Continued)

Table 2 (*Continued*)

	This study													Milella et al. (2021) (all human bones but one)
Area	ETH lab code	Sample code	Material	Treatment	Sample yield, %	%N in raw bone	%C in raw bone	%N in gelatin	%C in gelatin	mg C	C/N_{at}	^{14}C age BP	± 1σ	^{14}C age BP ± 1σ
21	105156	A21	Animal bone	UF1	1	5.46	17.59	18.8	42.2	0.32	2.6	*2030*	*24*	
	105157	W21	Wood	ABA	55					0.99		1753	23	
				Cellulose	35					0.99		1793	23	
				mean								***1773***	***16***	
	105158	H22	Human bone	UF1	4	5.63	17.81	16.6	45.5	0.99	3.2	1815	24	
				UF2	9			15.5	41.9	0.99	3.2	1793	22	
				mean								***1803***	***16***	
	105159	W22	Wood	ABA	N/A					1		1862	21	
22				Cellulose	5					1		1881	23	
				mean								***1871***	***16***	
	105160	A22	Animal bone	UF1	96	5.67	17.76	14.7	40.7	1	3.2	1816	22	
				UF2	9			16.2	44	0.99	3.2	1753	24	
				mean								***1787***	***17***	
	105161	H24	Human bone	UF1	3			15.8	43.2	1	3.2	1774	24	1755 ± 20
				UF2	9	5.66	17.67	13.4	36.1	0.99	3.1	1779	24	
				mean								***1776***	***17***	
24	105162	A24	Animal bone	UF1	2	5.698	17.6	14.8	41.1	0.99	3.2	*1832*	*22*	
	105163	W24	Wood	ABA	25					0.98		1809	23	
				Cellulose	15					1		1882	23	
				mean										
	105164	W32	Wood	ABA	N/A					0.99		1882	21	
				Cellulose	38					0.99		1890	23	
				mean								***1886***	***16***	
32	105165	H32	Human bone	UF1	3	5.63	18.02	13.4	37.7	0.99	3.3	1786	24	
				UF2	2			16.5	44.5	1	3.2	1786	24	
				mean								***1786***	***17***	
	105166	A32	Animal bone	UF1	2	5.58	17.62	16.1	44.7	0.99	3.2	***1861***	***22***	
	105167	W34	Wood	ABA	9					0.96		1713	21	
				Cellulose	2					0.09		0	0	
				mean								***1713***	***21***	

Table 2 (*Continued*)

	This study													Milella et al. (2021) (all human bones but one)
Area	ETH lab code	Sample code	Material	Treatment	Sample yield, %	%N in raw bone	%C in raw bone	%N in gelatin	%C in gelatin	mg C	C/N_{at}	^{14}C age BP	± 1σ	^{14}C age BP ± 1σ
34	105168	H34	Human bone	UF1	1	5.12	16.57	15.1	42.5	1	3.3	1774	24	1747 ± 19
														1716 ± 19
														1765 ± 20
				UF2	3			15.8	43.1	1	3.2	1755	24	1724 ± 19
				mean								***1765***	***17***	
	105169	A34	Animal bone	UF1	13	5.46	17.45	15.3	42.8	1	3.3	1542	21	
				UF2	7			16	43.4	1	3.2	1476	24	
				mean										
	105170	H40	Human bone	UF1	6	5.73	18.36	16.1	44.6	1	3.2	1768	24	
				UF2	7			16.3	44	1	3.1	1769	24	
				mean								***1768***	***17***	
40	105171	A40	Animal bone	UF1	12	5.31	17.25	16	44.3	0.99	3.2	1782	22	
				UF2	9			15.6	42.3	0.99	3.2	1736	24	
				mean								***1762***	***16***	
	105172	W40	Wood	ABA	N/A					0.92		1718	21	
				Cellulose	39					0.99		1735	23	
				mean								***1726***	***16***	
	105173	H42	Human bone	UF1	3	5.2	16.93	14.1	38.5	0.99	3.2	1766	24	1746 ± 20
				UF2	4			14.8	40.1	1	3.2	1754	24	
				mean								***1760***	***17***	
42	105174	A42	Animal bone	UF1	3	5.25	16.83	15.9	43.5	1	3.2	1766	24	
				UF2	7			16.5	44.7	1	3.2	1752	24	
				mean								***1759***	***17***	
	105175	W42*	Wood	ABA	55									
				Cellulose	81					0.08		—	—	
				mean										

elemental analyzer VarioMicroCube by Elementar (Nemec et al. 2010b; Wacker et al. 2010). Then the samples were subjected to AMS dating.

AMS Analysis and Radiocarbon Calibration

The measurements were performed at the ETH Laboratory of Ion Beam Physics in Zurich with the AMS system MICADAS (Synal et al. 2007), using oxalic acid (OXA II, SRM4990C{NIST}) for standard normalization and correction for isotope fractionation. Radiocarbon of pairs of treatment were evaluated. Coherent (2 sigma agreement) ages were combined and calibrated using OxCal v4.4.4 (Ramsey 2021) and an IntCal20 calibration data (Reimer et al. 2020). In addition in order to summarize the calibrated ages obtained in this study a Kernel Density Estimation (KDE) model function was used (Ramsey 2017).

RESULTS AND DISCUSSION

The measurement results of radiocarbon dating of this study, partially compiled with the previous results are listed in Table 2.

As mentioned in the "Preparation of Bones" section, the material for samples A18, A21, A24 and A32 was not available for repeated analysis and one sample of wood (W34) provided an insufficient amount of cellulose.

A comparison of ages obtained for various materials and methods showed that wood was more difficult to prepare than the bones, and human bones provided more consistent results than the animal bones. Six pairs of ABA and cellulose ages agreed within 2σ. The treatment with UF1 and UF2 resulted in coherent ages (2σ) for 9 human bones and 4 animal bones.

There is an interesting case of a very old animal bone A17 (ETH-105149) which provided coherent results for UF1 and UF2 that could be combined to 4194 ± 19 BP. The ages of wood pairs ranged in (1710–1886) ± 20 BP. This range is much wider than the ages of all bones (1753–1820) ± 17 BP. This is most likely due to the fact that the central archaeological structure under the amorphous stone accumulation was disturbed with a deep robber's pit at its center. The presence of water on the site made the documentation of the lower layers of the pit of structure 17 difficult. The old animal bone might have been part of a deeper soil layer dating to a time before the site experienced a surge in anthropogenic activity. The disturbance in combination with the high groundwater level might have caused these lower layers to mix.

For most of the samples, the UF1 and UF2 gelatine batches both gave satisfactory results in terms of the C/N atomic ratios (3.2–3.3). Sample A18 (ETH-105152) revealed a higher C/N_{at} ratio (3.5) and sample A21 (ETH-105156) was clearly an outlier with the C/N_{at} value of 2.6.I In both cases, these are animal bones and the ^{14}C ages are older than the majority, centered between 1750-1820 BP. Both samples were subjected only to UF1 preparation and it is difficult to say if UF2 would improve the result.

Although most of the bones showed high N% (~5%), the gelatine yield, based on >30kDa ultrafiltered fraction, is between 1–13%, which provides information about the degree of preservation (van Klinken 1999). For example, H34, despite the content of N=5.12% and C=16.57%, revealed a low gelatine yield in both UF1 and UF2 protocols (1 and 3%, respectively). A similar situation occurred with many other bone samples, for example H17,

https://doi.org/10.1017/RDC.2021.100 Published online by Cambridge University Press

H22 or A24—they showed right content of C and N, also C/N_{at} ratio was adequate but the sample yield was low after both pretreatment procedures. The wood samples also showed poor preservation of cellulose and only ABA treatment of whole wood resulted in high yield. For example, W17 ABA preparation resulted in 70% sample yield and Cellulose preparation—only in 17%. Similarly, W18_3 after ABA and Cellulose yielded 50% and 4% results, respectively, while the content of cellulose should reach 40–45% in coniferous species and 38–49% in deciduous species (Rowell 2005). Such was the case with most of wood samples (see Table 2).

Only the combined (i.e., coherent within 2 sigma) ages were calibrated with the exception of the animal bone A17 (ETH-105150) which is a clear outlier. The calibration program OxCal 4.4.4 (Ramsey 2021) was used with the INTCAL20 calibration data set (Reimer et al. 2020). The compilation of calibration plots is presented in Figure 3. In the next step the significantly older wood samples W22 and W32 were excluded and the KDE model was applied as shown in Figure 4. The KDE model considers the shape of the calibration curve while estimating the distribution of the events. The pool of radiocarbon ages obtained mostly on bones dates most of the monuments of the southern periphery of Tunnug 1 between the 2nd and 4th centuries CE, the date established by Milella et al. (2021).

A representation of all the data (this study and Milella et al. 2021) by a KDE model (Figure 4B) strengthens the conclusion of the rather short time interval between 200 and 400 CE, centered at 300 CE representations. A more precise calendar age might be prevented by the prominent wiggle on the calibration curve. Moreover, it might be noted that a sufficient pool of data is helpful when the possible outliers are present but not explained such as the old animal bone A17. The excellent agreement with the results of the radiocarbon dating by the Bern LARA laboratory demonstrates that modified ultrafiltration methods are comparable. The UF method applied by LARA lab (Szidat et al. 2017) to the Tunnug 1 bones has a significantly longer demineralisation step i.e., 60 hr as compared to max 2 hr in UF1/UF2. Indeed, the results of LARA show less scatter, which could be due to this step, or because all the bones were human bones. This study observed that animal bones in Tunnug 1 result in larger scatter.

Another observation is the difficulty to date wood. Some samples such as W42 dissolved during both treatments (ABA and Cellulose) and some, such as W34, survived ABA. One must note that the poor quality of decomposed wood is not striking from visual observation. In our study, ABA preparation provided at least as reliable results as Cellulose preparation. Such finding is important because decomposed, low-quality wood, is often encountered in archaeological material and application of ABA preparation is the only possibility. Moreover, ABA preparation is easier to carry out, and consumes less time and chemicals (especially $NaClO_2$, which is poisonous and carcinogenic) than BABAB preparation.

CONCLUSIONS

The main goal of our study was to evaluate the reliability of treatment methods. The original task of testing the bone treatment against the ages obtained on wood became impossible due to the poor cellulose preservation. Although ABA and Cellulose BABAB treatment of wood samples returned consistent results for the majority of samples, the BABAB preparation turned out to be less efficient than ABA, due to the low material yield after chemical preparation. The cellulose obtained was also of poor yield which resulted in a shift in the measurement result. We conclude that ABA is the effective method when dating poorly

https://doi.org/10.1017/RDC.2021.100 Published online by Cambridge University Press

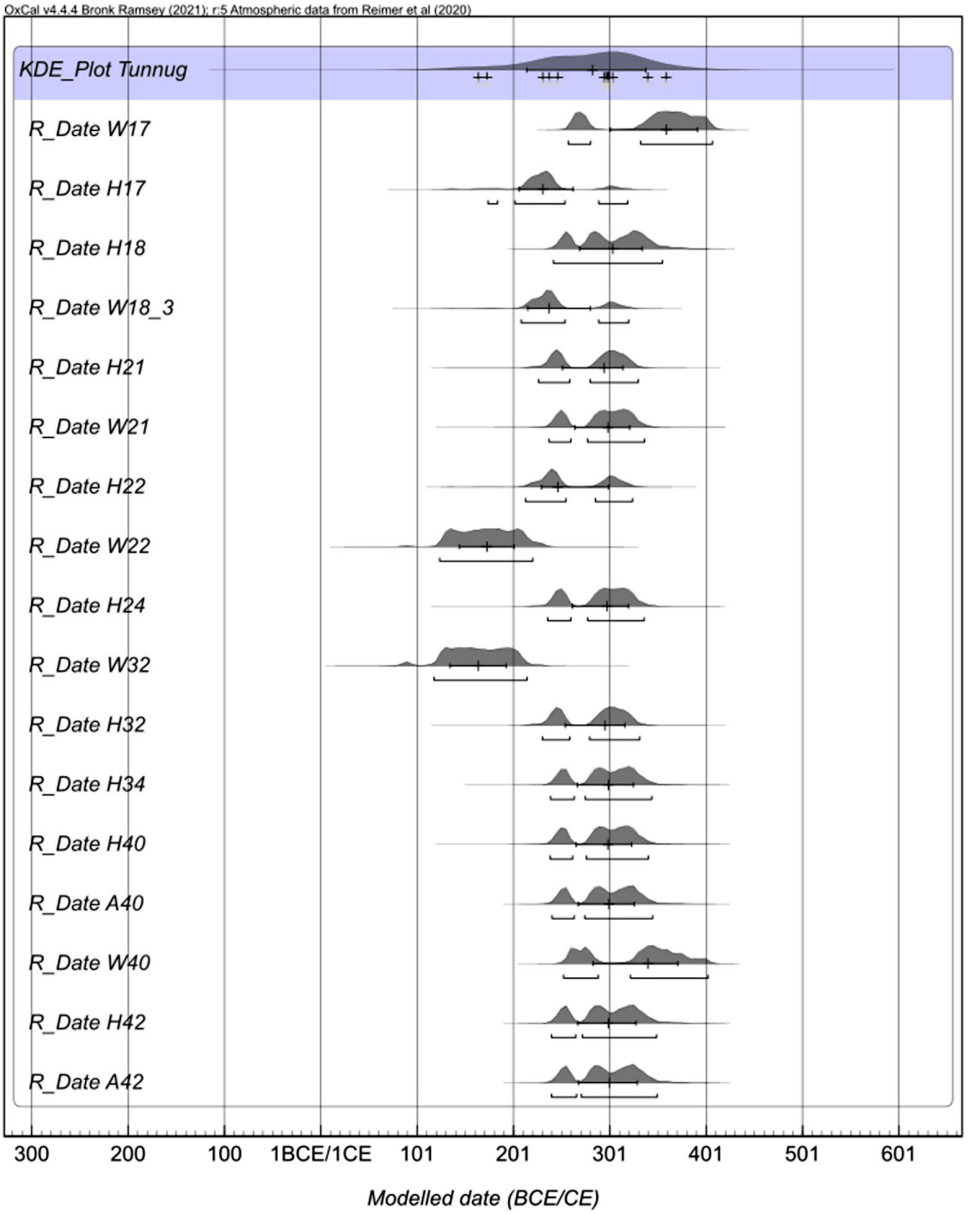

Figure 3 Multiple plot of calibrated radiocarbon ages obtained on human bones (H), animal bones (A), and wood (W). The sample numbers correspond to the archaeological structure. Ages of paired preparations (UF1 and UF2 for bones and ABA and Cellulose for wood) were combined when coherent (agreement at 2σ level).

preserved wood. The preparation of bones provided a more coherent picture. The results obtained by two modified ultrafiltration methods in this study suggested equal effectiveness in terms of the C/N_{at} values and gelatine purity. The critically evaluated paired ages of

https://doi.org/10.1017/RDC.2021.100 Published online by Cambridge University Press

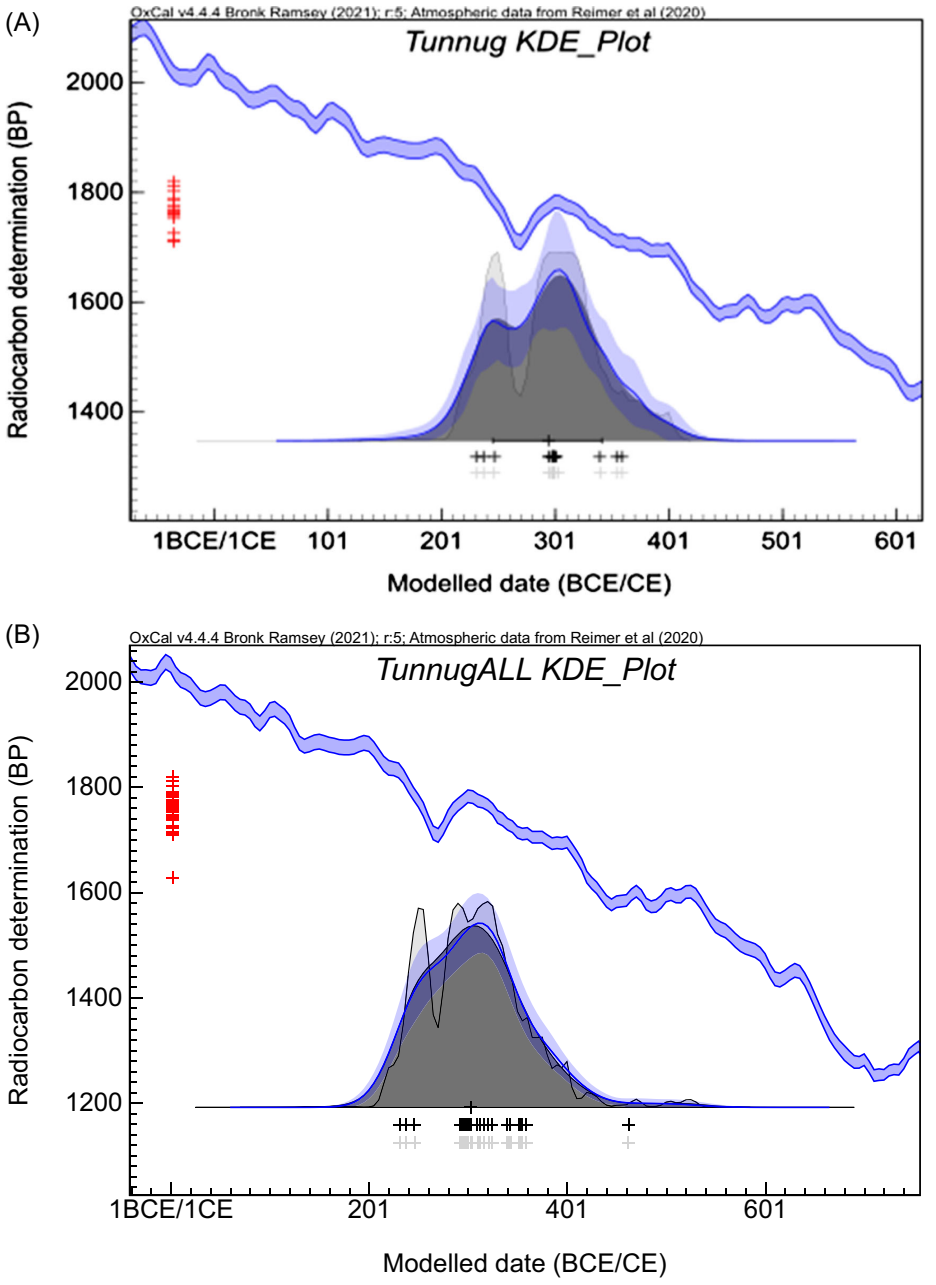

Figure 4 Plot showing the Kernel Density estimation model (KDE) for the Tunnug 1 data set obtained with OxCal 4.4.4. and INTCAL20 calibration curve: (A) this study; (B) this study combined with data from Milella et al. (2021). The gray solid curve (and light gray shading) shows unmodelled summed probability distributions (SPD), the blue solid curve and dark shaded area correspond to the Kernel Density results, with blue bands showing confidence interval around the kernel density estimate. The light shaded area corresponds to the sum distribution (Ramsey 2017). Red crosses are combined ^{14}C ages (Table 2, this study) and black/gray crosses show the median values of the calibrated likelihoods.

https://doi.org/10.1017/RDC.2021.100 Published online by Cambridge University Press

bones and wood support the chronology established by LARA laboratory and date the Kokel burials in the southern periphery of Tunnug 1 between 200 and 400 CE.

ACKNOWLEDGMENTS

Publication supported under the Excellence Initiative—Research University, The Silesian University of Technology, 2019 (03/FSW18/0003-04/2019). F. Pawełczyk would like to thank the staff of the ETH Laboratory of Ion Beam Physics in Zurich for their kind welcome, valuable tips and help at every stage of the works. Field research was conducted as a joint expedition of the Institute of the History of Material Culture of the Russian Academy of Sciences, the Russian Geographical Society (project "Expedition Tunnug") and the Swiss ArchaeoExploration. The excavation project is conducted with the financial and logistical help of the Russian Geographical Society (N 53/04/2019) and financial help of Dr F. Paulsen, the Society for the Exploration of EurAsia and the Russian Ministry of Culture (project No. 656-01-1-41/12-18 and N 1205/12-20). Post-excavation works for T. Sadykov and J. Blochin were carried out within the framework of the Program of Fundamental Scientific Research of the Russian Academy of Sciences, State Assignment No. 0184-2019-0011. G. Caspari was funded by the Swiss National Science Foundation, grant number P400PG_190982.

REFERENCES

Ambrose SH. 1990. Preparation and characterisation of bone and tooth collagen for isotopic analysis. Journal of Archaeological Science 17:431–451.

Arslanov KA, Svezhentsev YS. 1993. An improved method for radiocarbon dating fossil bones. Radiocarbon 35(3):387–391.

Brock F, Ramsey CB, Higham T. 2007. Quality assurance of ultrafiltered bone dating. Radiocarbon 49(2):187–192.

Brock F, Higham T, Ditchfield P, Ramsey CB. 2010. Current pretreatment methods for AMS radiocarbon dating at the Oxford Radiocarbon Accelerator Unit (ORAU). Radiocarbon 52: 103–112.

Brock F, Higham T, Bronk Ramsey C. 2010. Pre-screening techniques for identification of samples suitable for radiocarbon dating of poorly preserved bones. Journal of Archaeological Science 37:855–865.

Brown TA, Nelson DE, Vogel JS, Southon JR. 1988. Improved collagen extraction by modified Longin method. Radiocarbon 30:171–177.

Caspari G. 2020. Mapping and damage assessment of "royal" burial mounds in the Siberian Valley of the Kings. Remote Sensing 12(5):773.

Caspari G, Sadykov T, Blochin J, Hajdas I. 2018. Tunnug 1 (Arzhan 0)—an early Scythian kurgan in Tuva Republic, Russia. Archaeological Research in Asia 15:82–87.

Caspari G, Sadykov T, Blochin J, Buess M, Nieberle M, Balz T. 2019. Integrating remote sensing and geophysics for exploring early nomadic funerary architecture in the "Siberian Valley of the Kings". Sensors 19(14):3074.

Caspari G, Sadykov T, Blochin J, Bolliger M, Szidat S. 2020a. New evidence for a bronze age date of chariot depictions in the Eurasian Steppe. Rock Art Research 37(1):53–58.

Caspari G, Blochin J, Sadykov T, Balz T. 2020b. Deciphering circular anthropogenic anomalies in PALSAR data—using L-band SAR for analyzing archaeological features on the Steppe. Remote Sensing 12(7):1076.

DeNiro MJ. 1985. Postmortem preservation and alteration of in vivo bone collagen isotope ratios in relation to palaeodietary reconstruction. Nature 317(6040):806–809.

Deviese T, Comeskey D, McCullagh J, Bronk Ramsey C, Higham T. 2018. New protocol for compound-specific radiocarbon analysis of archaeological bones. Rapid Communications in Mass Spectrometry 32:373–379.

de Vries HL, Barendsen GW. 1954. Measurements of age by the carbon-14 technique. Nature, 174(4442), 1138–1141.

Fiedel SJ, Southon JR, Taylor R, Kuzmin YV, Street M, Higham TF, van der Plicht J, Nadeau M-J, Nawalade-Chavan S. 2013. Assessment of interlaboratory pretreatment protocols by radiocarbon dating an elk bone found below Laacher See tephra at Miesenheim IV (Rhineland, Germany). Radiocarbon 55:1443–1453.

Fuller BT, Fahrni SM, Harris JM, Farrell AB, Coltrain JB, Gerhart LM, Ward JK, Taylor RE, Southon JR. 2014. Ultrafiltration for asphalt removal from bone collagen for radiocarbon dating and isotopic analysis of

Pleistocene fauna at the tar pits of Rancho La Brea, Los Angeles, California. Quaternary Geochronology 22:85–98.

Hajdas I, Hendriks L, Fontana A, Monegato G. 2017. Evaluation of preparation methods in radiocarbon dating of old woods. Radiocarbon 59:727–737.

Hajdas I, Michczynski A, Bonani G, Wacker L, Furrer H. 2009. Dating bones near the limit of the radiocarbon dating method: study case mammoth from Niederweningen, Zh Switzerland. Radiocarbon 51:675–680.

Heinemeier KM, Schjerling P, Heinemeier J, Magnusson SP, Kjaer M. 2013. Lack of tissue renewal in human adult Achilles tendon is revealed by nuclear bomb ^{14}C. FASEB Journal 27: 2074–2079.

Herrando-Pérez S. 2021. Bone need not remain an elephant in the room for radiocarbon dating. Royal Society Open Science 8(1):201351.

Higham TF, Jacobi, RM, Ramsey CB. 2006. AMS radiocarbon dating of ancient bone using ultrafiltration. Radiocarbon 48(2):179–195.

Hogg A, Turney C, Palmer J, Southon J, Kromer B, Ramsey CB, Boswijk G, Fenwick P, Noronha A, Staff R, Friedrich M, Reynard L, Guetter D, Wacker L, Jones R. 2013. The New Zealand kauri (*Agathis australis*) research project: a radiocarbon dating intercomparison of Younger Dryas wood and implications for IntCal13. Radiocarbon 55:2035–2048.

Huels M, van der Plicht J, Brock F, Matzerath S, Chivall D. 2017. Laboratory intercomparison of Pleistocene bone radiocarbon dating protocols. Radiocarbon 59(5):1543–1552.

Kuzmin YV, Fiedel SJ, Street M, Reimer PJ, Boudin M, van der Plicht J, Panov VS, Hodgins GWL. 2018. A laboratory inter-comparison of AMS ^{14}C dating of bones of the Miesenheim IV elk (Rhineland, Germany) and its implications for the date of the Laacher See eruption. Quaternary Geochronology 48:7–16.

Longin R. 1971. New methods of collagen extraction for radiocarbon dating. Nature 230(5291): 241–242.

Marom A, McCullagh JS, Higham TF, Sinitsyn AA, Hedges RE. 2012. Single amino acid radiocarbon dating of Upper Paleolithic modern humans. Proceedings of the National Academy of Sciences 109:6878–6881.

McCullagh JS, Marom A, Hedges RE. 2010. Radiocarbon dating of individual amino acids from archaeological bone collagen. Radiocarbon 52:620–634.

Milella M, Caspari G, Kapinus Y, Sadykov T, Blochin J, Malyutina A, Keller M, Schlager S, Szidat S, Alterauge A, Lösch S. 2021. Troubles in Tuva: patterns of perimortem trauma in a nomadic community from Southern Siberia (second to fourth c. CE). American Journal of Physical Anthropology 174:3–19.

Nelson DE. 1991. A new method for carbon isotopic analysis of protein. Science 251:552–554.

Nemec M, Wacker L, Hajdas I, Gaggeler H. 2010a. Alternative methods for cellulose preparation for AMS measurement. Radiocarbon 52(3): 1358–1370.

Nemec M, Wacker L, Gäggeler HW. 2010b. Optimisation of the graphitisation process at AGE-1. Radiocarbon 52(3):1380–1393.

Olsen J, Heinemeier J, Hornstrup KM, Bennike P, Thrane H. 2013. "Old wood" effect in radiocarbon dating of prehistoric cremated bones? Journal of Archaeological Science 40(1):30–34.

Piotrowska N, Goslar T. 2002. Preparation of bone samples in the Gliwice radiocarbon laboratory for AMS radiocarbon dating. Isotopes in Environmental and Health Studies 38:267–275.

Quarta G, Molnár M, Hajdas I, Calcagnile L, Major I, Jull AJT. 2021. ^{14}C intercomparison exercise on bones and ivory samples: implications for forensics. Radiocarbon 63(2):533–544.

Ramsey C. 2021. OxCal 4.4. Electronic document.

Ramsey CB. 2017. Methods for summarizing radiocarbon datasets. Radiocarbon 59(6):1809–1833.

Reimer PJ, Austin WEN, Bard E, Bayliss A, Blackwell PG, Bronk Ramsey C, Butzin M, Cheng H, Edwards RL, Friedrich M, Grootes PM, Guilderson TP, Hajdas I, Heaton TJ, Hogg AG, Hughen KA, Kromer B, Manning SW, Muscheler R, Palmer JG, Pearson C, van der Plicht J, Reimer RW, Richards DA, Scott EM, Southon JR, Turney CSM, Wacker L, Adolphi F, Büntgen U, Capano M, Fahrni SM, Fogtmann-Schulz A, Friedrich R, Köhler P, Kudsk S, Miyake F, Olsen J, Reinig F, Sakamoto M, Sookdeo A, Talamo S. 2020. The IntCal20 Northern Hemisphere radiocarbon age calibration curve (0–55 cal kBP). Radiocarbon 62(4):725–757.

Rowell RM. 2005. Handbook of wood chemistry and wood composites. CRC Press.

Rubinetti S, Hajdas I, Taricco C, Alessio S, Isella LP, Giustetto R, Boano R. 2020. An atypical medieval burial at the Monte Dei Cappuccini monastery in Torino (Italy): a case study with high-precision radiocarbon dating. Radiocarbon 62(2):485–495.

Sadykov TR, Caspari G, Blochin J. 2019. The Early Scythian Burial mound Tunnug 1: Preliminary results of the excavation of the southern periphery [Раннескифский курган Туннуг 1: результаты первых работ на южной периферии памятника]. Theory and Practice of Archaeological Research 25:29–38.

Sadykov T, Caspari G, Blochin J. 2020. Kurgan Tunnug 1—new data on the earliest horizon of Sythian material culture. Journal of Field Archaeology, 1–15.

Sadykov T, Caspari G, Blochin J, Lösch S, Kapinus Y, Milella M. 2021. The Kokel of southern Siberia:

https://doi.org/10.1017/RDC.2021.100 Published online by Cambridge University Press

New data 1 on a Post-Xiongnu material culture. In press.

Scott EM, Cook GT, Naysmith P. 2010. A report on phase 2 of the Fifth International Radiocarbon Intercomparison (VIRI). Radiocarbon 52:846–858.

Southon JR, Magana AL. 2010. A comparison of cellulose extraction and ABA pretreatment methods for AMS ^{14}C dating of ancient wood. Radiocarbon 52:1371–1379.

Synal H A, Stocker M, Suter M. 2007. MICADAS: a new compact radiocarbon AMS system. Nuclear Instruments and Methods in Physics Research Section B: Beam Interactions with Materials and Atoms 259(1):7–13.

Sveinbjörnsdóttir ÁE, Heinemeier J, Arneborg J, Lynnerup N, Ólafsson G, Zoëga G. 2010. Dietary reconstruction and reservoir correction of ^{14}C dates on bones from pagan and early Christian graves in Iceland. Radiocarbon 52:682–696.

Szidat S, Vogel E, Gubler R, Lösch S. 2017. Radiocarbon dating of bones at the LARA laboratory in Bern, Switzerland. Radiocarbon 59(3): 831–842.

van Klinken GJ. 1999. Bone collagen quality indicators for palaeodietary and radiocarbon measurements. Journal of Archaeological Science 26:687–695.

Wacker L, Nemec M, Bourquin J. 2010. A revolutionary graphitisation system: fully automated, compact and simple. Nuclear Instruments and Methods in Physics Research B 268(7–8):931–934.

Wood R. 2015. From revolution to convention: the past, present and future of radiocarbon dating. Journal of Archaeological Science 56:61–72.